



iJRASET

International Journal For Research in
Applied Science and Engineering Technology



INTERNATIONAL JOURNAL FOR RESEARCH

IN APPLIED SCIENCE & ENGINEERING TECHNOLOGY

Volume: 12 Issue: IV Month of publication: April 2024

DOI: <https://doi.org/10.22214/ijraset.2024.60174>

www.ijraset.com

Call:  08813907089

E-mail ID: ijraset@gmail.com

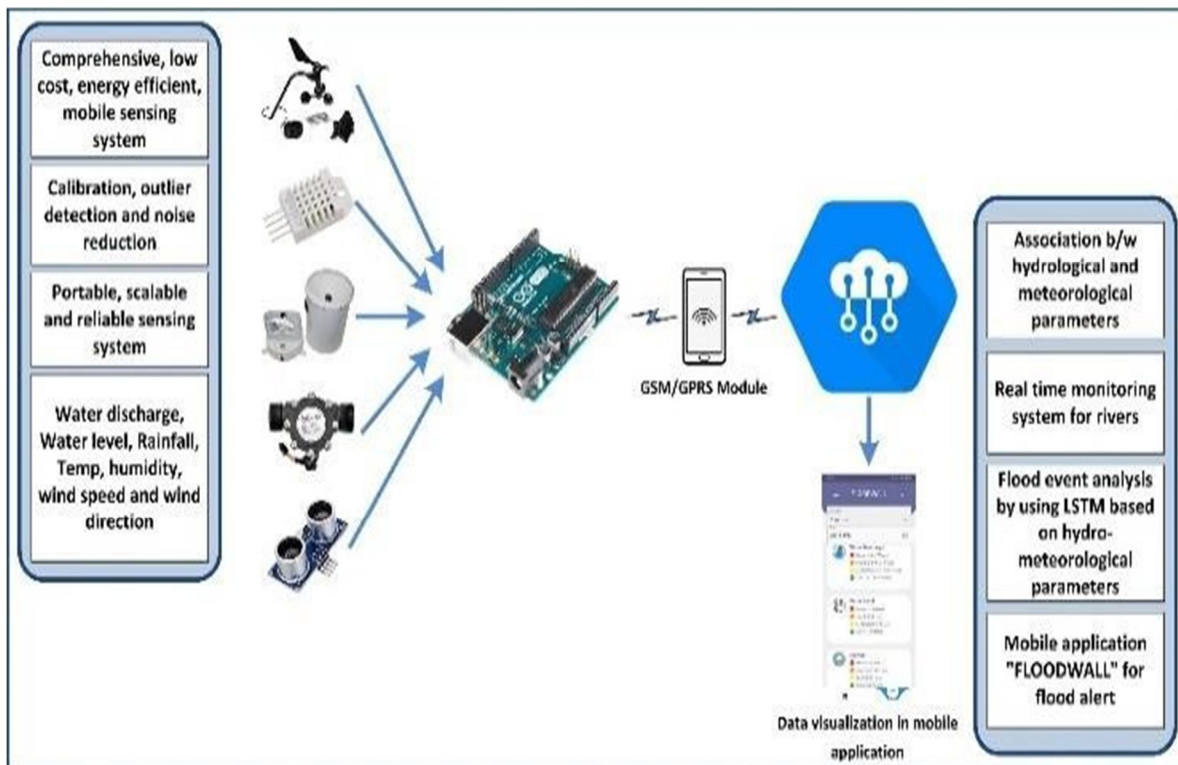
"FLOODGUARD: An IoT-Powered Real-Time Flash Flood Monitoring and Forecasting System"

Mr. P. Venkanna¹, D. Prasannakumar², V. Aravind³, K. Raviteja⁴, P. Seshanjaneyulu⁵

¹Assistant Professor, ^{2,3,4}Student, Department of Electronics and Communication Engineering, Usha Rama College of Engineering and Technology, Telaprolu, Ungunturu Mandal, Krishna, Andhra Pradesh, India

Abstract: In recent times, the surge in flooding incidents has become a pressing global issue, inflicting extensive damage on both lives and livelihoods. While floods remain an inevitable force of nature, their devastating impact can be alleviated. With the aid of cutting-edge technologies like the Internet of Things (IoT), proactive flood forecasting has become increasingly feasible. Through the seamless integration of IoT data, populations can receive early warnings and evacuate to safety, safeguarding both lives and valuables. A real-time solution is imperative, leveraging IoT data streams to deliver timely flood alerts. Our study presents an IoT-driven prototype designed to collect hydrological data from rivers, encompassing metrics such as water flow, level, and discharge, alongside meteorological parameters like temperature, humidity, wind speed, and direction. Employing a Long Short-Term Memory (LSTM) model, we analyze and classify collected data based on water discharge, level, rainfall, and temperature, predicting flood events as "no alert," "yellow alert," "orange alert," or "red alert." Given the dynamic nature of rivers, accurately measuring total water discharge poses challenges. To address this, we propose a novel methodology utilizing water flow, sectional area width, and average depth. Furthermore, we tackle the complexities associated with accurately measuring rainfall due to erratic weather conditions. Our system demonstrates robust performance in predicting flood event states, achieving high FI-scores of 97% for "no alert," 97% for "yellow alert," 96% for "orange alert," and 98% for "red alert."

Index Terms: Rapid inundation surveillance, hydro-climatic data, IoT-enabled systems, LSTM network, energy-efficient, rainfall and river data, sensor alignment, discharge rate, aquatic elevation.



I. INTRODUCTION

In everyday language, when human lives are at risk due to any naturally occurring event, that situation is commonly referred to as a natural calamity. Nature's fury, including thunderstorms, cyclones, tornadoes, floods, flash floods, droughts, seismic events, landslides, and avalanches, wreak havoc, causing harm to property and inflicting human casualties, as well as economic setbacks [1]. Roads sustain severe damage, large structures crumble, bridges fail, vehicular mishaps abound, and comparable devastations occur as a result of these catastrophic events. It poses a formidable challenge... for governmental and administrative bodies to bounce back from the damages incurred by the calamities. Inundation emerges as a foremost challenge [2] experienced in diverse locations worldwide. A flood arises when there is an excessive rise in water levels, such as when snow melts excessively [3]. While these calamities cannot be eradicated, the profound damage they cause can be mitigated. Disaster mitigation, encompassing both structural and nonstructural measures, is imperative to safeguard human lives and assets from natural calamities. It includes a thorough assessment of the damage caused by disasters, restoration of communication channels, transportation and rescue, water intake, and restoration of electric power to the affected areas [1]. One of the pivotal strategies within the realm of nonstructural approaches to disaster mitigation is to alert the populace prior to the onset of the calamity. Accordingly, plans for rescue operations are also formulated.

The state of Uttarakhand, situated in northern India, has not been spared from the impact of natural calamities. This Himalayan region, with its distinct geological characteristics, has experienced formations, environmental conditions, and climatic fluctuations, is frequently susceptible to natural calamities, notably floods, landslides, and earthquakes. In 2013, inundations in Kedarnath, Uttarakhand, resulted in catastrophic devastation, claiming the lives of over 6000 individuals. Flood disasters have had a very adverse effect on the life of the people of Uttarakhand in the last few decades [3]. Moderate or torrential rains from mid-June to September. (i.e., monsoon) come as a problem for the people here. The livelihoods of individuals in this mountainous region are severely disrupted by floods, resulting in loss of life and property. Agricultural land, as well as public infrastructure including roads, bridges, and educational facilities, suffer damage. The damage caused by floods can be mitigated through the implementation of appropriate measures.

It is essential to identify the flood-prone areas, so that proper arrangements can be made. Whether it is flood prediction or early warning systems based on thresholds in India, this achievement would not have been attainable without the contributions of the India Meteorological Department (IMD) and the Central Water Commission (CWC). The IMD offers meteorological or weather forecasts, while the CWC furnishes flood predictions at multiple river sites. Consequently, the efficacy of flood prediction systems hinges on the timeliness of weather forecasts provided by the IMD and how quickly. The majority of flood forecasts in India is based on old statistical techniques that have a lead time of less than 24h. Between the base station and the forecast station, these statistical techniques fail to receive the hydrological data of the river basins.

A. Our Contribution

Floods result in losses to human lives, property, and the environment. Therefore, there is a need for assessing of floods with regards to sustainable development. The achievements of the present study are delineated as follows.

A holistic, cost-effective, energy-conserving, portable sensing system is proposed, delivering instantaneous and continuous information. Calculating the overall water discharge poses challenges due to the dynamic geographic characteristics of the rivers. To address this challenge, an innovative approach for computing water discharge based on water flow, sectional area width and sectional average depth is proposed. Sudden and swift alterations in the sensor's operational surroundings impact the sensor output values. Consequently, the projected output deviates from the actual output. Sensor calibration facilitates enhancing sensor precision and performance.

Calibration and anomaly detection techniques have been utilized to minimize prediction discrepancies. For the creation of a real-time flood prediction system, simultaneous availability of hydrological and meteorological data is essential. The proposed system offers a distinctive aspect in its method for establishing correlation.

Between hydrological and meteorological parameters to predict the flash flood. Given the dynamic geographic attributes of rivers in hilly regions, the present study has been conducted to investigate the portability, scalability, and reliability of the sensing system to collect the data. A forecast model is built using long short-term memory (LSTM) technique, and its performance is thoroughly assessed using metrics such as root mean square error (RMSE) and precision, recall, and F1-score, which has been further compared with existing systems in the literature to validate the model.

II. RELATED WORK

The domains of application for the Internet of Things (IoT), sensing, analysis, and modeling of flash flood have been discussed in some of the recent works. Hart and Martinez [7] explored how IoT can transform a conventional wireless sensor network (WSN) to connect the world of things, which can provide seamless connections to connect the world of things, which can provide seamless connections, water quality, radiation pollution, and agriculture systems. Sandro et al. [9] present an efficient digitization process for improvements and effective use of limited resources, process, and system by using IoT-supported smart technologies. Minghu and Li [10] proposed a low-cost and high-speed data collection system across hard-to-reach areas by using IoT-enabled drone, based on 5 GHz and long range (LoRa) technology. To tackle challenges such as cost, time consumption, and power consumption associated with air quality monitoring stations, Jalpa and Mishra [11] suggested the IoT-integrated environmental monitoring system. In [12], a river flood surveillance, modeling, and forecasting methodology by scrutinizing the physical processes of the river. Shi-Wei et al. [13] proposed an image-based monitoring system for flood occurrence and analysis of water-level changes. They have used a camera for visual sensing of river water level. Mustafa et al. [14] (PIR) sensors that can continuously monitor water level and remote temperature, respectively. A combination of artificial neural network (ANN) and L1-regularized reconstruction are used to process measurement data. Prachatos et al. [15] proposed a model to collect the data by using WSN network, which has been implemented by using a modified mesh network over ZigBee, and to send the data over the Internet, a general packet radio service (GPRS) module is used. Gustavo et al. [16] have developed a fault-tolerant embedded system to detect and forecast the occurrence of flood based on WSN, IoT, and machine learning (ML) named as SENDI and evaluated on ns-3.

Jayashree et al. [17] explored various flood forecasting methodologies and introduced a flood warning system, addressing the limitations identified in the reviewed systems. Kun et al. [18] conducted flood detection through IoT and dispatched alert messages to end users, containing information on water level conditions and flow over time. Shah et al. [19] devised a flood alert mechanism capable of measuring river water levels and the rate of increase, enabling early notifications via short message service (SMS). Abdullahi et al. [20] integrated flow sensor, water-level sensor, and pressure gauge to gather data and assess flood conditions using a two-class neural network on Microsoft's Azure ML. Qundus et al. [21] introduced a flood detection system to collect data such as precipitation, temperature, humidity, water level, wind speed, and air pressure from sensors, monitoring variations in weather conditions compared to historical data. Kumar et al. [22] engineered an IoT system to collect rainfall and water level data, employing an expert system to analyze data for flood risk assessment. Mendoza-Cano et al. [23] developed an IoT-based flood monitoring system for hydrometeorological data, including weather parameters, soil moisture, and water level. Kitagami et al. [24] proposed a resilient network based on an event-driven data collection mechanism and feedback control system for real-time flood alerts. Sunkpho and Ootamakorn [25] established real-time water condition monitoring using WSN, employing mobile GPRS communication to transmit measured data to the server. Ghapar et al. [26] suggested an IoT system for flood data management, facilitating IoT infrastructure development for collecting, transmitting, and managing flood data. Dragulinescu et al. [27] proposed a smart IoT platform to monitor neighborhoods, issuing alerts to residents and responding to emergencies in their building or nearby structures. Basnyat et al. [28] outlined a design approach and detailed architecture for three distinct types of IoT-based flash flood detection systems.

A. Research Gaps

Existing studies have not sufficiently explored the monitoring and analysis of hydrological and meteorological parameters. There is a lack of research on identifying the most suitable, cost-effective, and energy-efficient sensors, microcontroller boards, communication modules, and cloud architectures for constructing a prototype to sense and analyze environmental parameters. While flood monitoring facilities are abundant in urban areas, there is a dearth of such facilities for populations residing in adjacent areas, along riverbanks, and in hilly regions. Limited attention has been given to calibration, outlier detection, and noise reduction methods for preprocessing sensed data. Research has yet to investigate the portability, scalability, and reliability of sensing devices. Hence, the impetus behind developing a comprehensive, cost-effective, energy-efficient, mobile sensing system based on IoT technology to monitor and forecast flash flood events and related parameters

III. ARCHITECTURE OF THE PROPOSED IOT SYSTEM

To oversee and report flood-like scenarios, there's a necessity for a system that endures extended periods and remains operational in remote regions with limited resources. To tackle these challenges, the proposed IoT architecture, illustrated in Fig. 1, incorporates a variety of inexpensive and energy-efficient sensors linked to a microcontroller. These sensors transmit collected data to the IoT cloud, where it undergoes further analysis, and users can access the information via an Android application.

This system actively monitors, gathers, stores, analyzes, and presents data in real-time. Hydrometeorological data are stored and analyzed in the IoT cloud.

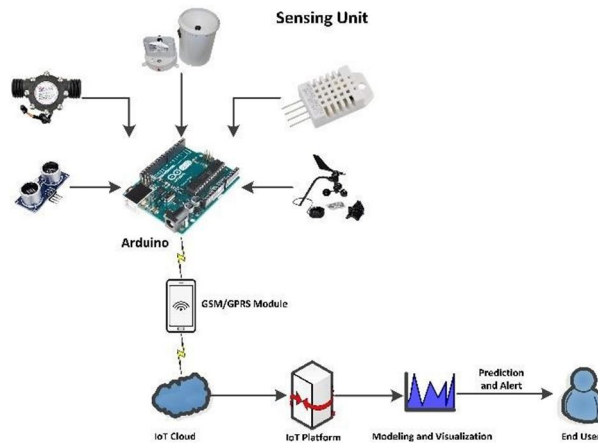


Fig. 1. IoT architecture for collection, storage, monitoring, and analysis of data

We have used an open-source, portable, energy-efficient, reconfigurable, and scalable board that comprises of an ATmega328p microcontroller, Arduino UNO [29]. This board offers the advantage of onboard power supply regulation, facilitating voltage regulation without the need for additional circuitry. It is compatible with a wide range of sensors and other components. The YF-S201 [30] water flow sensor is employed to monitor water volume and flow rate. HC-SR04 [31] ultrasonic sensors serve as a gauge to measure the distance (water level) between the sensor and the water surface. A tipping bucket [32] mechanism is utilized to measure rainfall at any given time. The connection between the tipping bucket and Arduino is established through the RJ11 connector. A cup anemometer [33] is a physical device employed to measure wind speed and direction. For communication, the SIM800L GSM module is utilized to transmit sensor data to the Google cloud. Table I provides specifications of the sensors utilized in our sensor configuration

A. Software Architecture and Data Communication

Conventional sensing stations for hydrological parameter measurement typically utilize costly instruments deployed at fixed locations. These stations often lack the capability to offer detailed and context-aware hydrological and meteorological data. Fixed stations also struggle to capture fine-grained data on hydrological changes due to the dynamic behavior of rivers. To overcome this limitation, we have implemented a resilient software architecture designed to seamlessly integrate with the hardware components of our proposed IoT system [34]. Table II provides an overview of the software applications utilized in our proposed system.

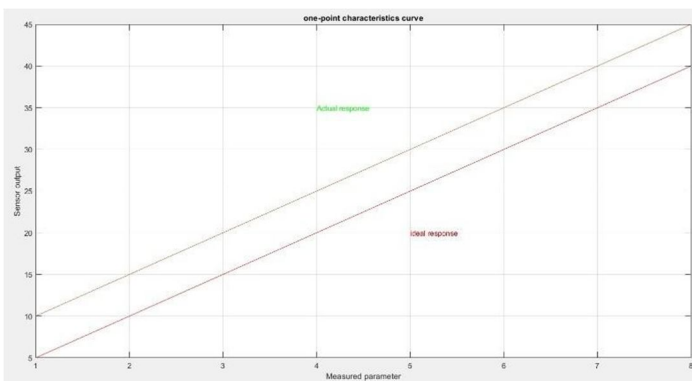


Fig. 2. One-point calibration characteristic curve with calibration offset.

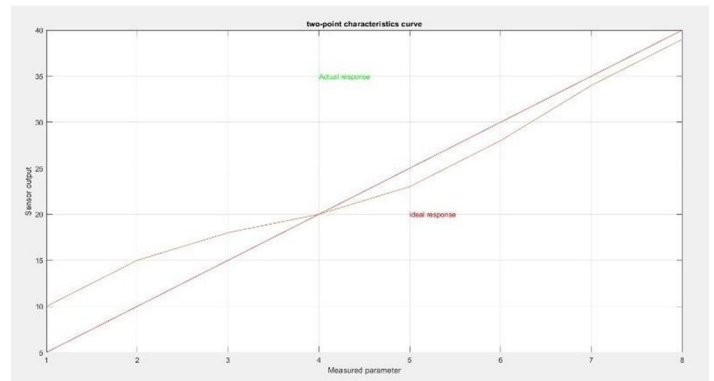


Fig. 3. Two-point calibration characteristic curve with calibration offset.

B. Calibrating Sensors

Changes in the working environment affect the sensors. Unwanted output values are produced by sudden and rapid changes in the sensor’s operating environment [36]. As a result, the predicted output differs from the actual output. Sensor calibration aids in the improvement of sensor accuracy and performance.

- 1) *Methods of Calibration Used:* Before we can understand these strategies, we must first understand the idea of a characteristic curve [37]. A characteristic curve is a graph that depicts a sensor’s reaction to a specific input value compared to its ideal linear response during the calibration procedure. The offset value indicates whether the sensor output exceeds or falls short of the ideal linear response
- 2) *Calibration using one-point scale:* When sensor output is linear and single level of precision measurement is required [37], a one-point calibration is employed to rectify sensor offset errors. Sensors for temperature are typically calibrated to a single point. Fig. 2 shows the one-point calibration characteristic curve with calibration offset.

A standard physical reference is taken for an instrument like a ruler and a meter stick in case of ultrasonic sensors, for distance. One reading is recorded from the reference instrument as reference value (V_R) and one measured sensor value (V_S); then, offset (O_R) is calculated

$$O_R = V_R - V_S$$

Now, the calibrated value (C_V) can be calculated by adding the offset to every reading received from the sensor

$$C_V = V_S + O_R$$

- 3) *Calibration using two-point scale:* Both offset and slope are corrected using two-point calibration. When the sensor determines that the output is linear across the measurement range, this calibration technique can be employed [37]. Fig.3 shows a two-point calibration characteristic curve with calibration values.

The readings are recorded from the reference instrument as reference low (R_l) and reference high (R_h), which are the low end and high end of the measurement range, respectively. Two measurements with the sensor are taken as: raw low (W_l) and raw high (W_h), which indicates the low end and high end of the measurement range, respectively. The raw range (W_r) and the reference range (R_r) are calculated as

$$R_r = R_h - R_l$$

$$W_r = W_h - W_l$$

Now, if the sensor recorded value is R_V , then calibrated value (C_V) after two-point calibration can be calculated as

$$C_V = (((R_V - W_l) * R_r) / W_r) + R_l$$

C. Power Consumption

To calculate battery backup time (BT) in hours [38], we require total load (LW) occupied by all components, battery capacity (BC), and input voltage (VB)

$$BT = BC * \frac{VB}{LW}$$

The Arduino Uno board uses 5-V input voltage and consumes 50-mA current. Arduino Uno power consumption (CA)

$$CA = 5 \times 50 = 250 \text{ mW}$$

TABLE I
COMPARISON OF DIFFERENT RAIN GAUGE TECHNOLOGIES

Features Technologies	Power Consumption	Measurement Capacity (feet)	Telemetry Support (Yes/No)	Accuracy (per feet)
Float Switch [44]	Magnetic 220V/500mA	Cable attached	Yes	4000-5000 ±3 mm 100*200
Ultrasonic [45]	Acoustic 5V/15mA	14	Yes	50-100 ±1 mm 45*20*15
Pressure [46]	Hydrostatic 5V/20mA	3-250	Yes	10000-15000 ±2 mm 140 mm long
Capacitive [47]	Capacitance 12-32V/30mA	6.50	Yes	7000-10000 ±0.1 mm 2000 mm long
Radar [48]	Pulse Radar 16V/50mA	115	Yes	82000-120000 ±3 mm 585*86

consumption by YF-S201 (CYF) and HC-SR04 (CHC) is

$$CYF = 5 \times 15 = 75 \text{ mW}$$

$$CHC = 5 \times 15 = 75 \text{ mW}$$

Most power consuming component in our proposed model is the tipping bucket rain precipitation sensor. This is rated at 12 V, 500 mA, but we have changed its reed switch and customized the buckets, so that power consumption can be reduced. After customization, power consumption is reduced to 5 V, 353 mA. Hence, power consumption by tipping bucket rain precipitation sensor (CTB) is

$$CTB = 5 \times 353 = 1765 \text{ mW}$$

The anemometer uses 12-V input voltage and 2 mA of current. Hence, power consumption by anemometer (CAM) is calculated as

$$CAM = 12 \times 2 = 24 \text{ mW.}$$

We have used the SIM800L GSM/GPRS module for communication, which is rated at 3.3 V, 453 mA, while using GPRS mode. Its power consumption (CG) can be calculated as

$$CG = 3.3 \times 453 = 1495 \text{ mW}$$

Required load (LW) (in watt) by the proposed prototype with all connected components can be calculated as

$$\frac{CA + CYF + CHC + CTB + CAM + CG}{1000}$$

$$\frac{250 + 75 + 75 + 1765 + 24 + 1495}{1000}$$

We have two rechargeable 12-V (VB), 12-AH sealed batteries, which are connected in parallel.

D. Cloud Infrastructure

For every seamless data collection device based on IoT, it is important to uniformly aggregate the data coming from different sensors, and this large amount of aggregated data must be stored in common format for processing. To store, process, analyze, and visualize on the large scale of data, we have used Google Cloud Platform (GCP) [39]. GCP provides services for computation, storage, networking, big data, ML, and IoT, as well as cloud management, security, and developer tools. Google's data services include data processing and analytics. In our system, we have used Google Cloud Dataflow (GCD) service for data processing facility and Google Cloud IoT Core service to access and manage data from IoT devices.

E. Sensors Details and Criteria

- 1) *DHT22*: The DHT22 temperature (T) and relative humidity (RH) sensor is chosen because it gives calibrated digital signal output. The DHT22 sensors are calibrated by the manufacturer in advance in a calibration chamber and the calibration coefficient is stored in the one-time-programmable (OTP) memory in program form. The sensing element is enabled with an 8-bit single-chip microcontroller. The sensor transmits 40 bits to the microcontroller: 16 bits for RH, 16 bits for temperature, and 8 bits for checksum [40].
- 2) *YF-S201*: The YF-S201 water flow sensor includes a rotor together with a Hall effect sensor inside a plastic body. When water passes through the sensor, it rotates the rotor, and the Hall effect sensor measures the pulse signal that was generated by the speed of the motor. Thus, the rate of water flow can be calculated [41]. The YF-S201 sensor is chosen because it is already manufacturer in advance and the calibration coefficient is stored in OTP memory in program form and adjusted while taking the readings. Let FR_m be the flow rate in milliliters and can be calculated as
- 3) *HC-SR04 Water Level*: In our proposed architecture, we In our proposed architecture, we A comparison of various level detection technologies is provided in Table III. The HC-SR04 ultrasonic sensor employs a transducer to transmit and receive ultrasonic pulses, which are used to ascertain the proximity of the water level. The sensor initiates an ultrasonic pulse at 40 kHz, which traverses through the air. If an object or obstacle is present, the sensor detects an echo. The distance can be calculated by measuring the travel time and the speed of sound [31].

TABLE II
COMPARISON OF DIFFERENT LEVEL DETECTION TECHNOLOGIES

				Telemetry Support (Yes/No)			
Symons Rain Gauge [49]	Manual	No power required	12.5 mm	No	1700-2700	±0.1 mm	30.5*12.7
Graduated Rain Gauge [50]	Manual	No power required	250 mm	No	1700-2550	±0.1 mm	50.8*20.32
Weighing Rain Gauge [50]	Mechanical	12V/9.2mA	Depend on drum size	Yes	35000-40000	±0.5 mm	67.7*45.5
Customized Tipping Bucket [51]	Automatic + Mechanical	5V/353mA	700 mm	Yes	8500-15000	±2.5 mm	34.2*20
Syphon (Float) type Rain Gauge [50]	Automatic	12V/10mA	600 mm	Yes	60000-80000	±3 mm	750*203
Optical Rain Gauge [50]	Automatic	12V/4mA	Continuous	Yes	25000	0.1 mm	121*71*56

F. Tipping Bucket

Various types of rain gauges are commercially available for measuring rainfall. However, it is imperative to select a rain gauge that is pre-calibrated, capable of continuous rainfall measurement, and cost-effective. To facilitate an informed decision, we conducted a comparative analysis of different rain gauges, presented in Table IV. Based on the comparison of properties and considering the climate conditions in India, we opted for the tipping bucket rain gauge in our proposed architecture. Additionally, we customized the gauge to minimize its power consumption. The tipping bucket operates via a reed switch that activates a transmitter. Subsequently, the receiver captures the radio frequency (RF) signal transmitted by the transmitter. This RF signal is then utilized by the microcontroller to compute and display rainfall data. During this process, the reed switch swiftly sends RF pulses, but the microcontroller's receiver receives RF pulses at a slower rate. The duration of the RF pulse is determined by the time it takes for the neodymium magnet to pass by the reed switch, which we have employed instead of a conventional magnet to enhance the reception rate of RF pulses while consuming less power [42]

G. Latency Analysis

Latency is the amount of time it takes to send data packets over a network. The sensed data are directly uploaded to the GCS IoT cloud. The GCS latency analysis dashboard provides the facility of notifying of any latency issues that the application programming interface (API) proxies are encountering. It shows latency metrics down to the minute level, emphasizing the median, 95th percentile, and 99th percentile values [43].

The median value indicates the value at which half of the traffic has latency more than this point and half of the traffic has latency less than this point. For example, if the median

The response processing time latency for an API proxy being 50 ms implies that half of its responses are completed in less than 50 ms, while the other half takes longer than 50 ms. The 95th percentile and 99th percentile values denote the latency thresholds at which 95% and 99% of the traffic experiences latency lower than these respective values. Furthermore, this analysis can identify outlier behavior, indicating that between 1% to 5% of the traffic is experiencing latency values outside of the expected range.

The GCS latency analysis dashboard offers four distinct latency metrics: response time, target response time, request processing latency, and response processing latency. Particularly, response processing latency represents the duration in milliseconds between the instance when the API proxy receives a response from the IoT gateway and when Apigee delivers the response to the Android app. Figure 4 illustrates the response processing latency over a 24-hour period.

IV. EXPERIMENTAL SETUP AND DATA COLLECTION

In this work, our mobile sensing setup is placed in three different subordinating rivers of the hillside areas of Uttarakhand, named as Tons, Song, and Nun rivers. The sensing setup was placed at the center of the river to closely monitor the status of the river from every angle. Here, the angle describes the water flow velocity, and it can be either fast due to the descent characteristic of the river or slow due to ascent characteristic of the river or normal due to evenness. The device is able to collect data seamlessly from June 2021 to present with a sampling rate of 1 sample/30 s. We have taken a small sampling rate because in fluvial and pluvial flash flood monitoring, it is required to monitor minor variations in river conditions. Fig. 5 demonstrates the physical placement of the data collection unit.

A. Flood Assessment Using Determination of Water Flow, Water Level, and RAINFALL (FLOODWALL)

The objectives of FLOODWALL are to provide a comprehensive real-time assessment of floods from all angles, indicating water discharge, which includes water flow or velocity, along with two additional parameters: water level and precipitation volume

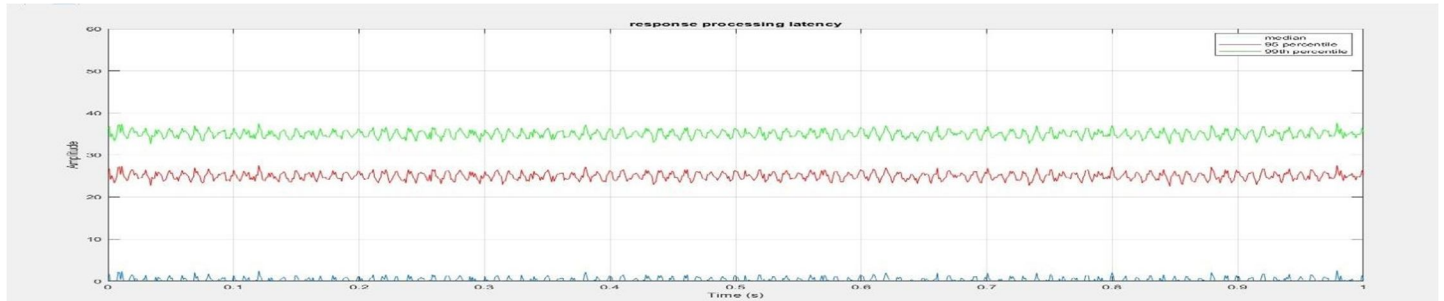


Fig. 4. Response processing latency of data receiving data. The median latency is indicated by blue line, 95th percentile by red line, and 99th percentile by green line.

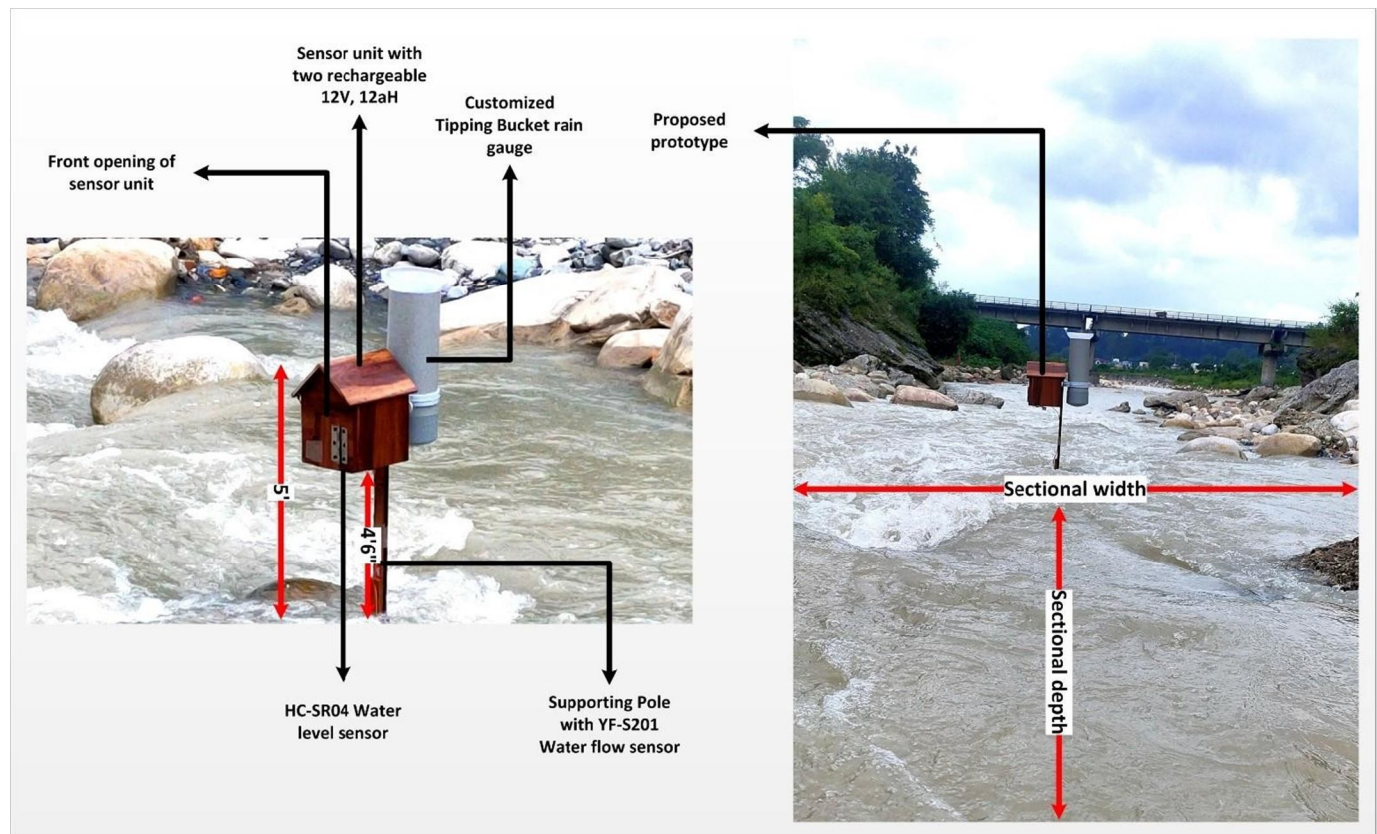


Fig. 5. Collecting sensor data from sensor node in real-time

B. Determination of Water Discharge

In an evolving environment, continuous stream flow combined with heavy precipitation serves as the primary catalyst for flooding. The dynamics of stream channels, such as the passage of water.

As water traverses the channel, the path and shape of the stream channel undergo continuous adjustments. Figure 6 illustrates a sectional area measurement demonstration. The discharge in a stream at any given point represents the volume of water passing through, typically measured in volume per unit time (m^3/s). The YF-S201 water flow sensor is employed to monitor the quantity of water passing through and the rate of water flow. The discharge (D) in m^3/s can be computed as follows

$$D = A * FR_m$$

where FR_m is the flow rate in milliliters derived from (9) and A is the sectional area of stream, which can be calculated as

$$A = W * D_{avg}$$

where W is the sectional area width and D_{avg} is the sectional area average depth

C. Determination of Water Level

Another essential parameter for flood assessment is the water level within the stream channel. Continuous monitoring of water level is imperative alongside water discharge, particularly during periods of heavy rainfall, such as the monsoon season. As discharge escalates in the stream channel over time, often due to heavy rainfall, there is a corresponding increase in water level. Therefore, it is crucial to

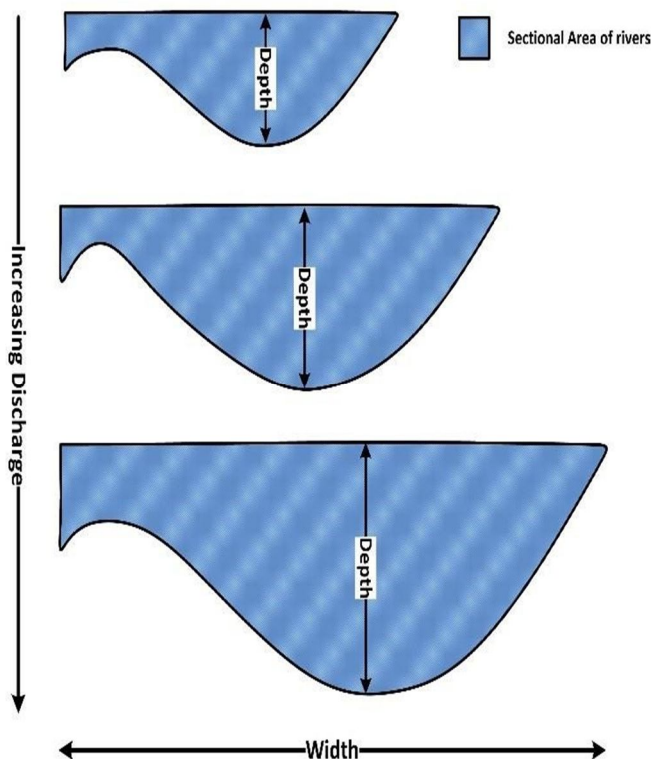


Fig. 6. Sectional area measurement.

continuously monitor the stream channel level. Let the surface of water be at 300 cm away from the sensor trigger and echo reflector, the pulse in the air travels with a speed of $0.034 \text{ cm}/\mu\text{s}$. This means that pulses need to travel (TP) in $8824 \mu\text{s}$, but the sensor doubles the distance as pulses travel forward and bounce backward to the sensor [31]. So, the distance (DWL) can be calculated as

$$DWL = \frac{0.034 * TP}{2}$$

D. Determination of Rainfall

In fact, in a span of three to four months, heavy rain results in increased flow of water in the rivers, which causes devastating floods. So, it is important to continuously monitor the total rainfall. In a rain event, at each tip per minute accumulated tip numbers are summed to the numbers of raw tipping bucket tips. Then, accumulated rainfall is calculated by multiplying total number of tips to gauge bucket size usually of 0.254 mm . To count the total rainfall more accurately and make it more suitable, interpolation methods, such as linear, quadratic, and cubic, can be used as the total rainfall is monotonous to the tips per minute. Simplest way to calculate the rain rate $[R(T_{n+1}) - T_n]$ between two consecutive tip minutes of gauge is a linear method

V. FORECAST MODELS

LSTM is an enhancement of the recurrent neural networks (RNNs). LSTM is best-suited to classify, process, and make forecasts based on time-series data. In order to solve the vanishing and the exploding gradient problem, LSTM

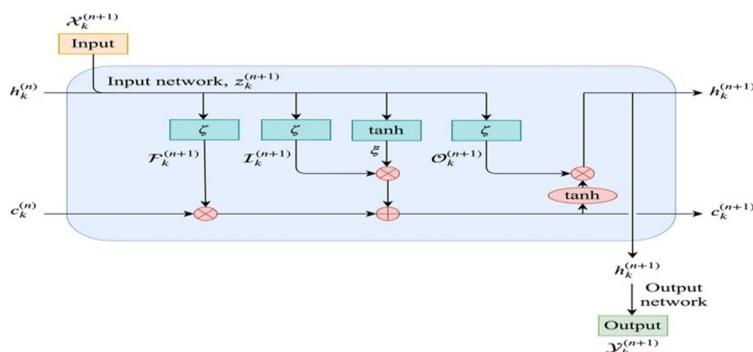


Fig. 7. Architecture of LSTM.

introduces blocks of memory in place of conventional RNN units. Unlike RNNs, in order to store long-term states, LSTM adds a cell state (S). An LSTM network remembers and links the information from the past with the current data [53]. As shown in Fig. 7, an LSTM consists of a cell and three gates, viz. input gate, forget gate, and output gate, where $ST - 1$ and ST represent the previous and the new cell states, respectively, XT corresponds to the current input, and OT and $O-T 1$ represent the new and previous outputs, respectively. Information is added to the cell state through the input gate. IT is obtained when the previous output $OT - 1$ and the current input XT are passed through the sigmoid layer.

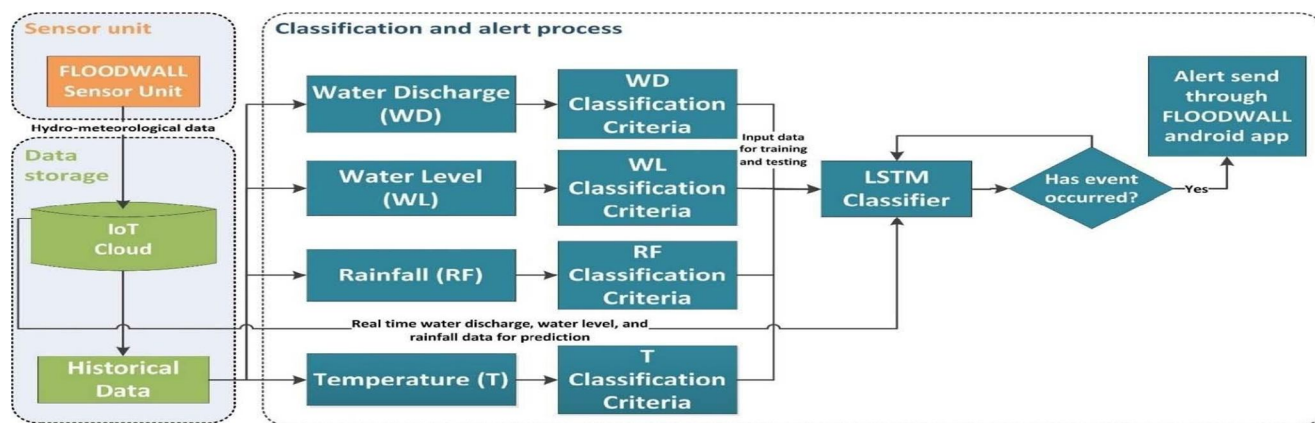


Fig. 8. Workflow diagram of flood classification system.

intermediate output \hat{Q} is multiplied with the new cell state ST after it is passed through the \tanh layer to obtain the final output

$$OT = \hat{Q} \tanh (ST).$$

The classifier output indicates if the test observation belongs to the no alert, yellow alert, orange alert, or the red alert class.

VI. DEVELOPMENT OF THE FORECAST MODEL

Water discharge, water level, precipitation, and temperature are the parameters utilized in flood modeling. Hydrological parameters are employed to assess variations in river conditions, while meteorological parameters are utilized to analyze changes in weather conditions at a specific geographic location. The system operates by deploying sensor nodes to capture both hydrological and meteorological data, as depicted in Fig. 8. The measured parameters serve as inputs to the LSTM model. The proposed system utilizes water discharge, water level, precipitation, and temperature as input parameters.

Water discharge is calculated using water flow. The LSTM algorithm is employed to detect flood occurrences at any given moment, utilizing water discharge, water level, precipitation, and temperature as inputs. It categorizes flood events into four levels: 1) no alert; 2) yellow alert; 3) orange alert; and 4) red alert. The model receives test observations from the sensor unit and determines flood occurrences based on LSTM analysis. In LSTM, the cells facilitate long-term memory incorporation in a more efficient manner by enabling the learning of additional parameters. This renders it the most potent neural network for prediction, particularly when our data exhibit a longer-term trend. The LSTM algorithm possesses a notable advantage over other machine learning algorithms. It can selectively learn, recall, or forget required historical data. It learns the outputs from the training data for the given features and predicts the outputs from the test data for the corresponding features [54].

The model takes inputs as water discharge, water level, rainfall, and temperature and computes real-time flood status as an output

VII. RESULTS AND DISCUSSION

The concentration of hydrological data is contingent upon time and location. The mountainous regions through which rivers flow are particularly vulnerable to flash floods. Therefore, to assess a developed model for real-time monitoring of various stream parameters, the hillside areas of Uttarakhand, India, have been chosen. The study entails an examination of water discharge, water level, and precipitation variations to gauge the occurrence of flash floods. Alongside these parameters, meteorological factors such as temperature, humidity, wind speed, and wind direction are also monitored to evaluate the influence of climate change on flood events. The primary objective of this endeavor is to provide early warnings to residents and facilitate their relocation to safer areas. To disseminate flood-related alerts to people seamlessly, a medium capable of continuously delivering information to the public is essential. To fulfill this requirement, we have developed a mobile application that offers easy access to flood-related information for individuals.

The application is divided into three different modules:

- 1) real-time sensors' data reporting;
 - 2) alert module; and
 - 3) historical and statistical information about the different parameters.
- Software technology is used to collect data from sensors, store it to the GCP, and send geo-targeted alerts to the individuals who are affected by the event through our mobile application "FLOODWALL." The FLOODWALL is a mobile application designed to retrieve data from the Google cloud by using APIs. Fig. 11 shows application screenshots, in which geotag on the map of three different locations is visible, and while clicking on the geotag, we can see the real-time data of different location parameters. Meanwhile, datewise location

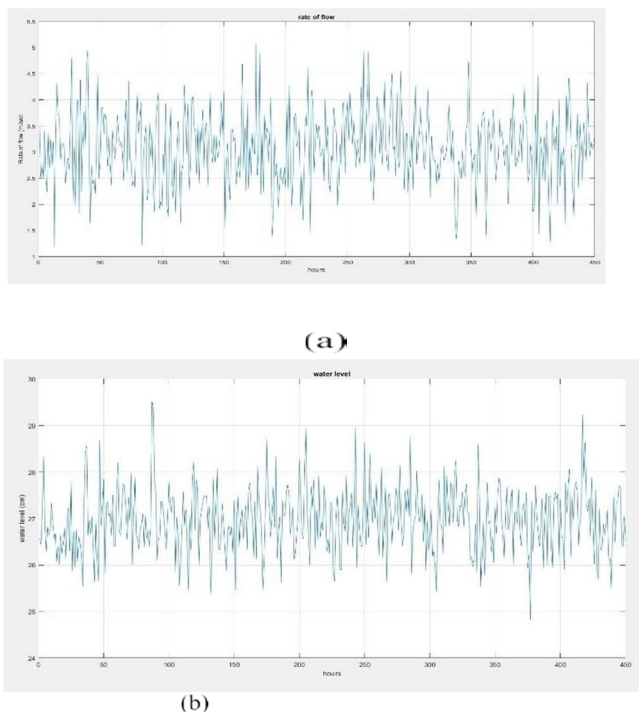


Fig. 9. (a) Variation of hourly water discharge. (b) Variation of hourly level.

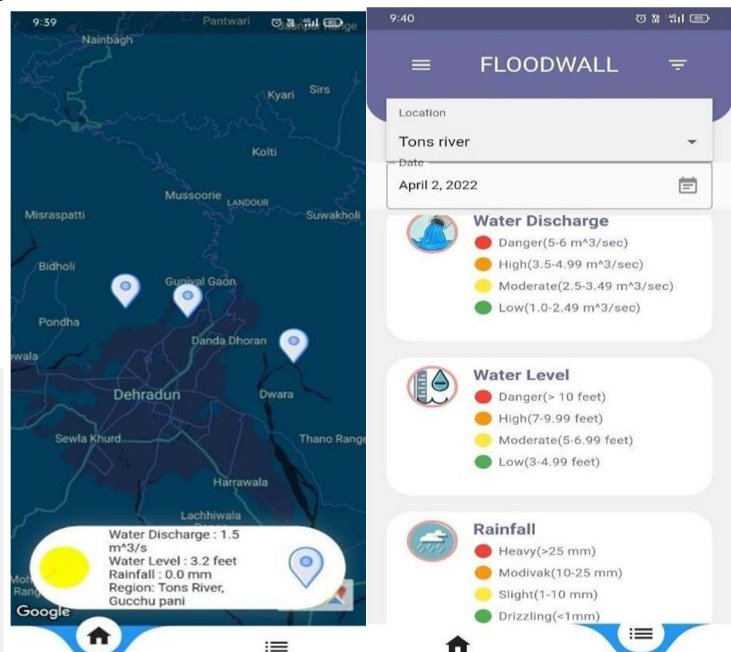


Fig. 11. FLOODWALL mobile application screenshots.

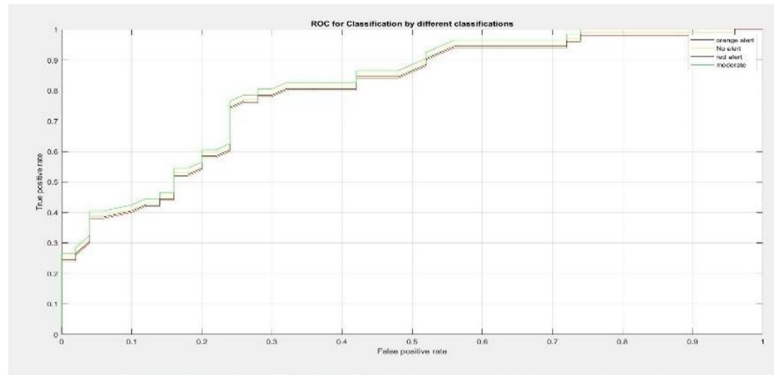


Fig. 11. ROC curve on events for different classification outcomes

specific information of different parameters is also available in the application. The application receives the updated data after every 5 min from the cloud. It shows the most recent hydrological and meteorological data, such as water discharge, water level, rainfall, temperature, humidity, wind speed, and wind direction. The application is able to show the data of three different rivers as per the user’s choice and selected date.

Since the sensors are already calibrated, the data coming from these sensors are accurate and correct. Furthermore, the alert module gives an alert to the user of the application and local authorities, when the values coming from the sensors exceed the predefined threshold values, configured in the system, through notifications.

The third module of the application is used for showing the historical and statistical information about the different parameters of the rivers in the form of graphs and charts. Fig. 9(a) and (b) shows the variation of hourly water discharge (calculated by taking sectional area of stream and water flow) and water level from September 15, 2021 to September 25, 2021. The data used for training and testing of the prediction model including the parameters, such as water discharge, water level, and rainfall, are based on a database that was built using the FLOODWALL device. Total 5919 experimental observations.

A. Area Under ROC

An ROC curve displays the sensitivity (TP rate) as a function of (1 - specificity) or the false alert ratio for various parameter threshold values. The ROC curve points provide a sensitivity pair for a certain decision threshold. The area under the curve (AUC) is a metric that measures a parameter’s ability to differentiate between different types of predicted classes.

shows the classification performance of the flood alert in the proposed model. The mean accuracy, precision, recall, and F1 scores for the red alert event are 99%, 98%, and 98%, respectively. The measures for orange alert incidents are 97%, 95%, and 96%, respectively. They are 97, 97, and 97, respectively, for the mild alert events. No threat event produces the best outcomes, with a TP rate of 99%, followed by moderate threat, threat with danger incidence, and high threat. The current model is quite accurate, with a mean F1 score of 0.97 for the four classes of the alert. The proposed model’s classification accuracy is illustrated clearly in Fig. 10 with the help of the ROC curve.

According to the flood alert ROC curve, the high alert event covers the most area, followed by the moderate alert, danger alert, and no alert events. The notifications are delivered to the user in the form of application alerts. The user receives notifications on their smartphone screen via the FLOODWALL Android application, which they need to install.

B. Model Validation

Several studies have reported the development of hardware and software solutions for analysis and detection of flash flood events; however, they are of limited use in establishing a comprehensive solution for flood disaster detection. This might be due to the coverage and integration of various geographies, climates, and data. Validation through comparison with another system is challenging; however, it may be possible by making use of different performance parameters of classification. To validate the prediction model’s effectiveness, three measures for classification performance (RMSE, correlation, and F1-score) have been used. Table VI shows the model validation through performance comparison with the existing systems. The developed classifier obtained an F1-score of 97% for “no alert,” 97% for “yellow alert,” 96% for “orange alert,” and 98% for “red alert,” which is clearly an improved prediction technique over other systems.

VIII. CONCLUSION

The research work carried out the development of a real-time monitoring system for rivers of the hillside area of Uttarakhand, India, to show the most recent hydrological and meteorological data, such as water discharge, water level, rainfall, temperature, humidity, wind speed, and wind direction. Furthermore, on the basis of the data received, the system generates an alert to the users and local authorities when the values coming from the sensors are predicted the status of the flood event by using LSTM model, through SMS and notifications. The proposed system is able to show historical and statistical information about different parameters of the rivers in the form of graphs and charts. Our low-cost and energy-efficient flood inundation IoT sensor unit is working on a sensor technology that monitors three remote flood-prone areas in real-time, where network availability is not so good. We have designed a mobile application "FLOODWALL" to retrieve data from the Google cloud by using APIs, which shows the most recent hydrological and meteorological data and generates an alert when the values coming from the sensors exceed the predefined threshold values, configured in the system through SMS and notifications. Our proposed system is successfully able to monitor regional pluvial and fluvial flood-related parameters since July 2021 and provide real-time flood-related information with 1 sample/30 s from three different remote locations. The sensors that we have used in our system are calibrated in advance and the data coming from these sensors are very much accurate and correct. The system works efficiently in terms of real-time data collection and end-user alerting. However, to increase the accuracy of flood forecasting, the proposed system can be integrated with geographic information systems and remote sensing technologies in future.

REFERENCES

- [1] L. Zhou, X. Wu, Z. Xu, and H. Fujita, "Emergency decision making for natural disasters: An overview," *Int. J. Disaster Risk Reduction*, vol. 27, pp. 567–576, Mar. 2018.
- [2] M. P. Mohanty, S. Mudgil, and S. Karmakar, "Flood management in India: A focussed review on the current status and future challenges," *Int. J. Disaster Risk Reduction*, vol. 49, Oct. 2020, Art. no. 101660.
- [3] S. Bisht, S. Chaudhry, S. Sharma, and S. Soni, "Assessment of flash flood vulnerability zonation through Geospatial technique in high altitude Himalayan watershed, Himachal Pradesh India," *Remote Sens. Appl., Soc. Environ.*, vol. 12, pp. 35–47, Nov. 2018.
- [4] A. Khanna and S. Kaur, "Internet of Things (IoT), applications and challenges: A comprehensive review," *Wireless Pers. Commun.*, vol. 114, no. 2, pp. 1687–1762, Sep. 2020.
- [5] Uttarakhand Disaster 2013. Accessed: Aug. 10, 2022. [Online]. Available: <https://nidm.gov.in/pdf/pubs/ukd-p1.pdf>
- [6] M. Ishiwatari, T. Koike, K. Hiroki, T. Toda, and T. Katsube, "Managing disasters amid COVID-19 pandemic: Approaches of response to flood disasters," *Prog. Disaster Sci.*, vol. 6, Apr. 2020, Art. no. 100096.
- [7] J. K. Hart and K. Martinez, "Toward an environmental Internet of Things," *Earth Space Sci.*, vol. 2, no. 5, pp. 194–200, May 2015. S. L. Ullo and G. R. Sinha, "Advances in smart environment monitoring systems using IoT and sensors," *Sensors*, vol. 20, no. 11, p. 3113, May 2020.
- [8] S. Nižetić, P. Šoljić, D. López-de-Ipiña González-de-Artaza, and L. Patrono, "Internet of Things (IoT): Opportunities, issues and challenges towards a smart and sustainable future," *J. Cleaner Prod.*, vol. 274, Nov. 2020, Art. no. 122877.
- [9] M. Zhang and X. Li, "Drone-enabled Internet-of-Things relay for environmental monitoring in remote areas without public networks," *IEEE Internet Things J.*, vol. 7, no. 8, pp. 7648–7662, Aug. 2020.
- [10] J. Shah and B. Mishra, "IoT-enabled low power environment monitoring system for prediction of PM2.5," *Pervas. Mobile Comput.*, vol. 67, Sep. 2020, Art. no. 101175.
- [11] G. Merkurjeva, Y. Merkurjev, B. V. Sokolov, S. Potryashev, V. A. Zelentsov, and A. Lektuers, "Advanced river flood monitoring, modelling and forecasting," *J. Comput. Sci.*, vol. 10, pp. 77–85, Sep. 2015.
- [12] S.-W. Lo, J.-H. Wu, F.-P. Lin, and C.-H. Hsu, "Visual sensing for urban flood monitoring," *Sensors*, vol. 15, no. 8, pp. 20006–20029, Aug. 2015.
- [13] M. Mousa, X. Zhang, and C. Claudel, "Flash flood detection in urban cities using ultrasonic and infrared sensors," *IEEE Sensors J.*, vol. 16, no. 19, pp. 7204–7216, Oct. 2016.
- [14] P. Mitra et al., "Flood forecasting using Internet of Things and artificial neural networks," in *Proc. IEEE 7th Annu. Inf. Technol., Electron. Mobile Commun. Conf. (IEMCON)*, 2016, pp. 1–5.
- [15] G. Furquim, G. Filho, R. Jalali, G. Pessin, R. Pazzi, and J. Ueyama, "How to improve fault tolerance in disaster predictions: A case study about flash floods using IoT, ML and real data," *Sensors*, vol. 18, no. 3, p. 907, Mar. 2018.
- [16] S. Jayashree, S. Sarika, A. L. Solai, and S. Prathibha, "A novel approach for early flood warning using Android and IoT," in *Proc. 2nd Int. Conf. Comput. Commun. Technol. (ICCCCT)*, Feb. 2017, pp. 339–343.
- [17] K. Han, D. Zhang, J. Bo, and Z. Zhang, "Hydrological monitoring system design and implementation based on IoT," *Phys. Proc.*, vol. 33, pp. 449–454, Dec. 2012.
- [18] W. M. Shah, F. Arif, A. A. Shahrin, and A. Hassan, "The implementation of an IoT-based flood alert system," *Int. J. Adv. Comput. Sci. Appl.*, vol. 9, no. 11, pp. 620–623, 2018.
- [19] S. I. Abdullahi, M. H. Habaebi, and N. A. Malik, "Intelligent flood disaster warning on the fly: Developing IoT-based management platform and using 2-class neural network to predict flood status," *Bull. Electr. Eng. Informat.*, vol. 8, no. 2, pp. 706–717, Jun. 2019.
- [20] J. Al Qundus, K. Dabbour, S. Gupta, R. Meissonier, and A. Paschke, "Wireless sensor network for AI-based flood disaster detection," *Ann. Oper. Res.*, pp. 1–23, Aug. 2020.
- [21] C. K. Khen and A. Zourmand, "Fuzzy logic-based flood detection system using lora technology," in *Proc. 16th IEEE Int. Colloq. Signal Process. Appl. (CSPA)*, 2020, pp. 40–45, doi: 10.1109/CSPA48992.2020.9068698.



- [22] O. Mendoza-Cano et al., "Experiments of an IoT-based wireless sensor network for flood monitoring in Colima, Mexico," *J. Hydroinformatics*, vol. 23, no. 3, pp. 385–401, May 2021.
- [23] S. Kitagami, V. T. Thanh, D. H. Bac, Y. Urano, Y. Miyanishi, and N. Shiratori, "Proposal of a distributed cooperative IoT system for flood disaster prevention and its field trial evaluation," *Int. J. Internet Things*, vol. 5, no. 1, pp. 9–16, 2016.
- [24] J. Sunkpho and C. Ootamakorn, "Real-time flood monitoring and warning system," *Songklanakar J. Sci. Technol.*, vol. 33, no. 2, pp. 1–15, 2011.
- [25] A. A. Ghapar, S. Yussof, and A. A. Bakar, "Internet of Things (IoT) architecture for flood data management," *Int. J. Future Gener. Commun. Netw.*, vol. 11, no. 1, pp. 55–62, Jan. 2018.
- [26] A.-M. Dragulinescu, A. Dragulinescu, C. Zamfirescu, S. Halunga, and G. Suci, "Smart neighbourhood: LoRa-based environmental monitoring and emergency management collaborative IoT platform," in *Proc. 22nd Int. Symp. Wireless Pers. Multimedia Commun. (WPMC)*, Nov. 2019, pp. 1–6.
- [27] B. Basnyat, N. Singh, N. Roy, and A. Gangopadhyay, "Design and deployment of a flash flood monitoring IoT: Challenges and opportunities," in *Proc. IEEE Int. Conf. Smart Comput. (SMARTCOMP)*, Sep. 2020, pp. 422–427.
- [28] Arduino R3 Documentation. Accessed: Aug. 22, 2022. [Online]. Available: <https://docs.arduino.cc/hardware/uno-rev3>
- [29] M. Arosio, C. Arrighi, L. Cesarini, and M. L. V. Martina, "Service accessibility risk (SAR) assessment for pluvial and fluvial floods in an urban context," *Hydrology*, vol. 8, no. 3, p. 142, Sep. 2021.
- [30] Č. Maksimović, D. Prodanović, S. Boonya-Aroonnet, J. P. Leitão, S. Djordjević, and R. Allitt, "Overland flow and pathway analysis for modelling of urban pluvial flooding," *J. Hydraulic Res.*, vol. 47, no. 4, pp. 512–523, Jul. 2009.



10.22214/IJRASET



45.98



IMPACT FACTOR:
7.129



IMPACT FACTOR:
7.429



INTERNATIONAL JOURNAL FOR RESEARCH

IN APPLIED SCIENCE & ENGINEERING TECHNOLOGY

Call : 08813907089  (24*7 Support on Whatsapp)